AAS 12-151

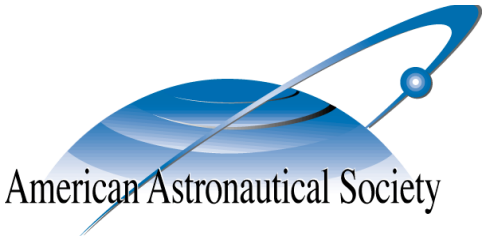

American Institute of
Aeronautics and Astronautics

STABILITY ANALYSIS AND OUT-OF-PLANE CONTROL OF COLLINEAR SPINNING THREE-CRAFT COULOMB FORMATIONS

Peter D. Jasch , Erik A. Hogan, and Hanspeter Schaub

AAS/AIAA Astrodynamics Specialists Conference

Charleston, South Carolina January 29–February 3, 2012

AAS Publications Office, P.O. Box 28130, San Diego, CA 92198

AAS 12-151

STABILITY ANALYSIS AND OUT-OF-PLANE CONTROL OF COLLINEAR SPINNING THREE-CRAFT COULOMB FORMATIONS

Peter D. Jasch*, Erik A. Hogan†, and Hanspeter Schaub‡

This paper analyzes the effects of out-of-plane perturbations on planar motion for collinear three-craft Coulomb formations with set charges. The formation is assumed to be spinning in deep space without relevant gravitational forces present. Previous work analytically proves marginal stability assuming in-plane motion with circular relative trajectories and the initial position and velocity perturbations confined to the orbital plane. In this paper, a new derivation of the equations of motion in cylindrical coordinates is produced to analyze the out-of-plane motion in more detail. The out-of-plane motion is shown to decouple to first order from the marginally stable in-plane motion. A control law is developed to maintain the out-of-plane motion within specified deadbands. For small relative out-of-plane perturbations, the control law succeeds in preserving the in-plane variant shape despite some out-of-plane motion. A trend between the settling time and deadband, which defines the largest out-of-plane errors allowed before the controller is turned on, is determined which illustrates how large the deadband may be before the in-plane motion is affected. A Monte-Carlo analysis also indicates that the spin-rate and formation size do not have a significant influence on the out-of-plane instability of a collinear invariant shape Coulomb formation.

INTRODUCTION

As the number of scientific missions venturing out into the Solar System and beyond increases, close formation flying of spacecraft proves to be the emerging technology that makes previously impossible missions become reality. With separation distances on the order of tens of meters, a formation of spacecraft may be used in applications in the fields of Earth imaging, advanced weather monitoring, planetary research, astronomy, and more.[3] Close-proximity spacecraft formations provide the freedom to place a large number of scientific instruments within a formation of satellites separated by tens of meters, rather than being limited to the space on a single satellite. Furthermore, the satellites in the formation may be placed into orbit upon separate launch vehicles. If a budget or time constraint exists, this aspect proves to be an advantage. As a result, a formation of this sort may be built over a period of time.

Electrostatic actuation using active charge control has been proposed as early as 1966, where it was suggested as a means to inflate a membrane structure in geosynchronous orbit altitudes.[4] In such space regions the local plasma results in very low Watt-level electrical power requirements and low Debye shielding effects. Later on starting in 2002 Coulomb formations are proposed that use electrostatic forces to maintain the shape of the spacecraft formation.[1,2] Attractive and repulsive

*Graduate Student, Department of Aerospace Engineering Sciences, University of Colorado
†Graduate Student, Department of Aerospace Engineering Sciences, University of Colorado
‡Associate Professor, H. Joseph Smead Fellow, Department of Aerospace Engineering Sciences, University of Colorado, AAS Member

forces are generated when charging individual spacecraft within the formation.[5] For constellations of satellites flying in close proximity, on the orders of tens of meters, small thrust levels on the order of micro-Newtons are needed from the propulsion system for formation maintenance. Furthermore, since sensitive scientific instruments onboard the satellites can easily be contaminated by caustic exhaust from traditional propellant-type thrusters, an electrostatic control system provides a means to control the spacecraft formation shape free from exhaust particles. As an active control system, it is very energy efficient, requiring power levels on the order of Watts.[6,7] Active charge control in space has been demonstrated on multiple missions.[8,9]

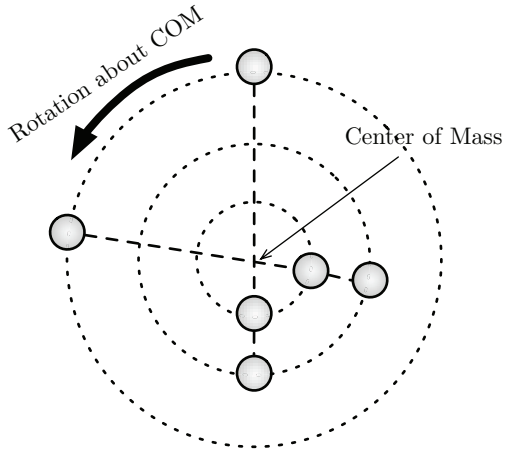

Figure 1. Collinear Three-Craft Invariant Shape Coulomb Formation

The current study considers collinear spinning three-craft invariant shape Coulomb formations in deep space as the spacecraft orbit about their collective center of mass in circular trajectories. This formation is depicted in Figure 1. Hussein and Schaub provide the theoretical foundation for determining invariant shape solutions for the three-craft Coulomb formation.[10] By specifying the craft charges, the collinear shape of the formation can be determined. Hogan and Schaub view the problem from a mission design perspective and solve for the craft charges when the collinear shape of the formation is specified.[11] It is proven that for any desired collinear invariant shape geometry, there exists a real charge solution. In fact, it is possible for up to three invariant shape solutions to exist for a single set of craft charges.[12] Through linear stability analysis, Reference 12 demonstrates that the in-plane motion may be marginally stable for the three-craft invariant shape formations in circular trajectories if particular formation geometrits are selected. This linear stability is only observed when two invariant shape solutions exist for a set of craft charges.[12] One solution is found to have unstable in-plane motion, while the other exhibits marginally stable rotational motion. This marginally stable configuration is a significant find in that it greatly simplifies the charged relative motion control of the three bodies. Earlier work only identified strongly unstable charged collinear configurations.[13,14] Further, prior to Reference 12, the only other passively stable charged relative motion configuration was the spinning charged two-body system discussed in Reference 15.

The study of invariant shape Coulomb formations is a special case of the more general charged three-body problem, which is, itself, an extension of the classical gravitational three-body problem as discussed in References 6, 16, and 17. Typically, the charged three-body problem considers the combined effects of gravitational and electrostatic forces on the motion of the bodies in the system. In the special case of invariant shape Coulomb formations, the relatively small masses of the

bodies (100s of kg) result in gravitational forces many orders of magnitude below the electrostatic forces. The lack of significant gravitational forces is actually a limitation on the system, as fewer forces are available to stabilize a relative geometry. In Reference 16, for example, a non-planar relative equilibrium is made possible by the combined influence of gravity and electrostatics. In Reference 17, central configurations are identified for the charged three-body problem. Stability of these central configurations is investigated in Reference 16.

In the current study, the charged three-body problem is considered for the case where the masses are too small to contribute meaningful gravitational forces. That is, only electrostatic forces are assumed to be acting the bodies in the system. Collinear central configurations are the focus, where the craft orbit the center of mass of the formation on circular trajectories. The effects of motion outside of this orbit plane are considered, with attention paid to resulting instabilities. It is of interest to determine if this out of plane motion decouples from the in-plane motion. If this is the case, then it is likely that small out of plane perturbations will not destabilize the in-plane motion until the magnitude of these perturbations becomes significant. A simple control strategy is investigated to keep the out-of-plane motion within a small enough deadband such that out-of-plane motion does not couple into and destabilize the collinear central configuration.

BACKGROUND

Invariant Shape Solutions of Coulomb Formations

This paper analyzes the behavior of collinear invariant shape Coulomb formations consisting of three spacecraft. The three craft rotate about their center of mass in deep space. Similar to work done by References 10 and 12, by assuming nonexistent gravitational forces and perturbations, the only forces which the spacecraft experience are due to the inter-craft electrostatic forces.

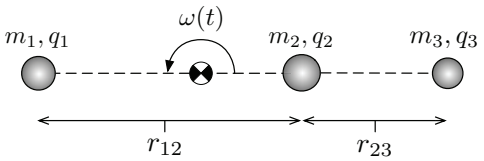

Figure 2. Collinear Invariant Shape Coulomb Formation[11]

The spacecraft are of mass m_i and charge q_i. For an invariant shape solution describing the formation geometry, the craft charges are assumed constant for all time. Each spacecraft has a position vector which describes the craft's location relative to the formation center of mass and is denoted by $\boldsymbol{r}_i$. The relative position vectors between spacecraft i and spacecraft j is denoted by $\boldsymbol{r}_{ij} = \boldsymbol{r}_j - \boldsymbol{r}_i$. An invariant shape Coulomb formation does not imply a fixed shape, as in constant inter-craft distances and constant distances between each craft and the center of mass. Rather, an invariant shape Coulomb formation implies a constant ratio of inter-craft distances. This is made clearer by consideration of the collinear formation depicted in Figure 2. As the craft orbit about the center of mass, the separation distances between the craft are allowed to vary as long as the ratio of the separation distances, χ, remains constant,

$$\chi = \frac{r_{23}}{r_{12}}. \tag{1}$$

It is important to note that χ will always be positive due to positive separation distances between the spacecraft. The collinear, invariant shape Coulomb formation orbits about its center of mass with the craft on Keplerian trajectories with a time-varying angular velocity $\omega(t)$.[10] The trajectories of the spacecraft may be circular, elliptic, parabolic, or hyperbolic while maintaining a collinear formation for all time.

In order to maintain an invariant shaped Coulomb formation, the three craft must possess specific charges. These charges are a function of the formation geometry and angular momentum (i.e. craft masses, craft angular velocity, and inter-craft separation distances). Thus, by specifying a set of craft charges, Hussein and Schaub[10] prove that the collinear formation geometry, χ, may be found by solving the quintic equation

$$\begin{aligned} 0 = &-c_2c_3(m_2+m_3) - c_2c_3(2m_2+3m_3)\chi \\ &+[c_1m_1(c_2-c_3) - c_2c_3(m_2+3m_3)]\chi^2 \\ &+[c_1c_2(3m_1+m_2) + c_3m_3(c_1-c_2)]\chi^3 \\ &+c_1c_2(3m_1+2m_2)\chi^4 \\ &+c_1c_2(m_1+m_2)\chi^5, \end{aligned} \tag{2}$$

where $c_i = q_i/m_i$ is the specific charge of each spacecraft. In comparison to Reference 11, Eq. (2) does not include the plasma-shielding electrostatic force. For initial analysis, this paper assumes a deep-space plasma condition where the effective Debye length is sufficiently large to make the plasma-related charge shielding negligible. By specifying the craft charges and masses, a total of six parameters, it is possible to determine solutions for χ. In real-world applications, a Coulomb formation mission would most likely be designed by specifying the formation geometry. The craft charges would then be solved for, as they are functions of the Coulomb formation geometry. This would require specifying the craft masses, formation spin rate, and χ, which would be followed by solving for the craft charges. The quintic equation in Eq. (2) allows for either case to be performed.

This paper assumes the three craft are of equal mass, m, and the Coulomb formation is operating in a space environment with large Debye lengths. The craft charge ratios are introduced as

$$\delta = \frac{q_1}{q_3}, \sigma = \frac{q_1}{q_2}. \tag{3}$$

These charge ratios allow the craft charges to be determined if one craft charge is assumed. From these definitions and assumptions, Eq. (2) simplifies to

$$0 = -2 - 5\chi + (\delta - \sigma - 4)\chi^2 + (4\delta + \sigma - 1)\chi^3 + 5\delta\chi^4 + 2\delta\chi^5. \tag{4}$$

The six total parameters which comprise Eq. (2) are reduced to two, δ and σ. Reference 12 examines the craft charge solution space in detail to find δ and σ values which yield multiple invariant shape solutions, χ.

To illustrate the concept of multiple invariant shape solutions in numerical results, Reference 12 uses charge ratios of $\delta = -0.05$ and $\sigma = 7$. This solution leads to two positive real roots of the quintic equation, χ values which determine two invariant shape solutions for Coulomb formations, $\chi = 3.2508$ and $\chi = 4.3283$. A linear stability analysis is then conducted to determine which of these χ solutions produce a stable spacecraft formation. It is found that the χ value of 3.2508 corresponds to an equilibrium exhibiting marginal stability while the χ value of 4.3283 results in an

unstable invariant shape. The current study investigates the marginally stable solution, $\chi = 3.2508$, in more detail in order to control the out-of-plane motion and create a stable spacecraft formation indefinitely.

Coulomb Formation Mean Motion and Orbital Period

Once the spacecraft charges are defined and an invariant shape solution obtained, the motion of the three spacecraft within the formation is determined. This section provides a brief summary of the invariant shape solution. Hussein et al[13] assumes the spacecraft motion is similar to a satellite's motion around a gravitational body. Within a Coulomb formation, the spacecraft orbit about the formation center of mass. The motion of each craft within a collinear invariant shape Coulomb formation is Keplerian and may be described by

$$\ddot{\boldsymbol{r}}_i = -\frac{\mu_i}{r_i^3}\boldsymbol{r}_i \tag{5}$$

where $\boldsymbol{r}_i$ is the vector from the formation center of mass to the individual craft i. In the orbital mechanics two body problem, μ_i is the effective gravitational parameter. In Eq. (5), it may be treated similarly, but it is important to note that its value is different for each craft. In orbital mechanics, μ is a function of the orbiting satellite's mean motion, n, and semi-major axis, a. The mean motion for each craft in a Coulomb formation is defined as a function of the effective gravitational parameter for a craft and the semi-major axis of the corresponding craft.

$$n = \sqrt{\frac{\mu_i}{a_i^3}}. \tag{6}$$

In the current application, the mean motion for all three craft must be equal in order to maintain a collinear invariant shape. For this reason, the effective gravitational parameter for only one craft is needed to find the mean motion for all spacecraft. The effective gravitational parameter for craft 1 is

$$\mu_1 = -\frac{k_c q_1}{\mathcal{M}_1}\left[q_2 e^{-r_{21}/\lambda_d} + \frac{q_3}{(1+\chi)^2}e^{-r_{31}/\lambda_d}\right], \tag{7}$$

where $k_c = 8.99$ x 10^9 Nm/C^2 is the Coulomb constant, and

$$\mathcal{M}_1 = \frac{m_1(m_1+m_2+m_3)^2}{m_2^2 + m_3^2(1+\chi)^2 + 2m_2m_3(1+\chi)}. \tag{8}$$

As previously stated, this paper assumes the spacecraft are of equal mass, m, and the formation is operating in deep space, meaning the Debye length, λ_d, is large. By applying these assumptions and the definitions of δ and σ from Eq. (3), Eq. (7) can be rewritten as

$$\mu_1 = -\frac{k_c q_1^2(2+\chi)^2}{9m(1+\chi)^2}\left[\frac{(1+\chi)^2}{\sigma} + \frac{1}{\delta}\right] \tag{9}$$

By using a predefined semi-major axis for craft 1, a_1, and the effective gravitational parameter for craft 1 calculated in Eq. (9), the mean motion for all three craft can be found with Eq. (6). The orbital period, P, of the formation is then defined as

$$P = \frac{2\pi}{n}. \tag{10}$$

Inertial Coulomb Formation Description

Reference 13 describes the motion of a Coulomb formation in an inertial frame while Reference 12 uses a rotating frame which is fixed to craft 1 to define the formation motion. One goal of this paper is to define a system of equations with respect to an inertial frame in cylindrical coordinates. By comparing the new cylindrical equations of motion with the inertial description from Reference 13, more insight into the formation motion may be obtained. A brief description of the inertial motion description follows.

For a collinear invariant shape Coulomb formation depicted in Figure 2, the craft are assumed point masses with position vectors relative to the center of mass defined as

$$\begin{aligned} \boldsymbol{r}_1 &= \pm\, r_1 \hat{\boldsymbol{e}}_1 \\ \boldsymbol{r}_2 &= \pm\, r_2 \hat{\boldsymbol{e}}_1 \\ \boldsymbol{r}_3 &= \pm\, r_3 \hat{\boldsymbol{e}}_1, \end{aligned} \tag{11}$$

where the $\boldsymbol{e}_1$ direction points from the formation center of mass to craft 3 at the initial time. In order to obtain an acceleration expression for each craft, derivatives are taken with respect to the inertial frame. By assuming deep space operation and nonexistent space weather, external forces are neglected. The spacecraft only experience forces due to the interaction between craft charges in the formation. Thus, the equations of motion for craft i is described as[18]

$$m_i \ddot{\boldsymbol{r}}_i = \boldsymbol{F}_i = \sum_{j=1, j\neq i}^{3} k_c \frac{q_i q_j}{r_{ij}^2} \hat{\boldsymbol{e}}_{\boldsymbol{ji}}, \tag{12}$$

where q_i and q_j are the charges of crafts i and j, respectively, r_{ij} is the distance between crafts i and j, and $\hat{\mathbf{e}}_{\mathbf{ji}}$ is the unit vector from craft j to craft i.

DYNAMICAL ANALYSIS

Cylindrical Equations of Motion

In order to gain further insight into the motion of collinear invariant shape Coulomb formations, this paper derives the previously stated inertial equations of motion in a cylindrical coordinate frame. This process begins by presenting the position vectors of each spacecraft in the Coulomb formation with respect to a cylindrical coordinate frame. The position of each craft is defined by a radius magnitude, r_i, representing the planar distance from the formation center of mass to the current craft i, an angle, θ_i, specifying the rotation between the inertial $\hat{\boldsymbol{e}}_1$ axis and the craft radius vector at the current time, and an out-of-plane component, z_i. In the cylindrical frame, the position of a craft i in the formation is given by

$$\boldsymbol{R}_i = [r_i \cos(\theta_i) \quad r_i \sin(\theta_i) \quad z_i]. \tag{13}$$

The acceleration expression in Eq. (12) is used to obtain the new equations of motion, which requires differentiation of Eq. (13) in order to obtain $\ddot{r}_i$ for each craft. After carrying out the required differentiation and substitution into Eq. (12), the equations of motion in cylindrical coordinates are

found to be

$$\ddot{r}_1 = \frac{k_c q_1 \left(r_1 \left(q_2 r_{13}^3 + q_3 r_{12}^3 \right) - q_2 r_{13}^3 r_2 \cos(\theta_1 - \theta_2) - q_3 r_{12}^3 r_3 \cos(\theta_1 - \theta_3) \right)}{m_1 r_{12}^3 r_{13}^3} + r_1 \dot{\theta}_1^2 \tag{14a}$$

$$\ddot{r}_2 = \frac{k_c q_2 \left(q_1 r_{23}^3 (r_2 - r_1 \cos(\theta_1 - \theta_2)) + q_3 r_{12}^3 (r_2 - r_3 \cos(\theta_2 - \theta_3)) \right)}{m_2 r_{12}^3 r_{23}^3} + r_2 \dot{\theta}_2^2 \tag{14b}$$

$$\ddot{r}_3 = \frac{k_c q_3 \left(q_1 r_{23}^3 (r_3 - r_1 \cos(\theta_1 - \theta_3)) + q_2 r_{13}^3 (r_3 - r_2 \cos(\theta_2 - \theta_3)) \right)}{m_3 r_{13}^3 r_{23}^3} + r_3 \dot{\theta}_3^2 \tag{14c}$$

$$\ddot{\theta}_1 = k_c q_1 \left(\frac{q_2 r_2 \sin(\theta_1 - \theta_2)}{m_1 r_1 r_{12}^3} + \frac{q_3 r_3 \sin(\theta_1 - \theta_3)}{m_1 r_1 r_{13}^3} \right) - \frac{2 \dot{r}_1 \dot{\theta}_1}{r_1} \tag{14d}$$

$$\ddot{\theta}_2 = k_c q_2 \left(\frac{q_3 r_3 \sin(\theta_2 - \theta_3)}{m_2 r_2 r_{23}^3} + \frac{q_1 r_1 \sin(\theta_1 - \theta_2)}{m_2 r_2 r_{12}^3} \right) - \frac{2 \dot{r}_2 \dot{\theta}_2}{r_2} \tag{14e}$$

$$\ddot{\theta}_3 = -k_c q_3 \left(\frac{q_1 r_1 \sin(\theta_1 - \theta_3)}{m_3 r_3 r_{13}^3} + \frac{q_2 r_2 \sin(\theta_2 - \theta_3)}{m_3 r_3 r_{23}^3} \right) - \frac{2 \dot{r}_3 \dot{\theta}_3}{r_3} \tag{14f}$$

$$\ddot{z}_1 = k_c q_1 \left(\frac{q_2 (z_1 - z_2)}{m_1 r_{12}^3} + \frac{q_3 (z_1 - z_3)}{m_1 r_{13}^3} \right) \tag{14g}$$

$$\ddot{z}_2 = k_c q_2 \left(\frac{q_1 (z_2 - z_1)}{m_2 r_{12}^3} + \frac{q_3 (z_2 - z_3)}{m_2 r_{23}^3} \right) \tag{14h}$$

$$\ddot{z}_3 = k_c q_3 \left(\frac{q_1 (z_3 - z_1)}{m_3 r_{13}^3} + \frac{q_2 (z_3 - z_2)}{m_3 r_{23}^3} \right). \tag{14i}$$

Linearization of Cylindrical Equations of Motion

The Coulomb formation is found to be marginally stable in Reference 12 for a specified set of formation parameters χ, δ, and σ. The in-plane motion of the Coulomb formation preserves its shape while the out-of-plane motion remains relatively small compared to the formation geometry. From this observation, it is hypothesized that the out-of-plane motion decouples from the in-plane motion for small deviations from the reference. To prove this hypothesis, the newly-developed cylindrical equations of motion are linearized. The equations of motion for the in-plane motion, $\boldsymbol{r}$ and $\boldsymbol{\theta}$, and out-of-plane motion, $\boldsymbol{z}$, is described in Eq. (14) and can also be written as

$$f_r(\boldsymbol{r}, \boldsymbol{\theta}, \boldsymbol{z}) = \begin{bmatrix} \ddot{r}_1 \\ \ddot{r}_2 \\ \ddot{r}_3 \end{bmatrix}, f_\theta(\boldsymbol{r}, \boldsymbol{\theta}, \boldsymbol{z}) = \begin{bmatrix} \ddot{\theta}_1 \\ \ddot{\theta}_2 \\ \ddot{\theta}_3 \end{bmatrix}, f_z(\boldsymbol{r}, \boldsymbol{\theta}, \boldsymbol{z}) = \begin{bmatrix} \ddot{z}_1 \\ \ddot{z}_2 \\ \ddot{z}_3 \end{bmatrix} \tag{15}$$

A reference state, ($\boldsymbol{r}_r$ $\boldsymbol{\theta}_r$ $\boldsymbol{z}_r$), must first be established which the equations of motion are linearized about. For a stable formation, the out-of-plane positions, velocities, and accelerations are zero, i.e. $\boldsymbol{z}_r = \dot{\boldsymbol{z}}_r = \ddot{\boldsymbol{z}}_r = 0$. For the in-plane reference motion, the radial positions are constant with zero velocities and accelerations, i.e. $\boldsymbol{r}_r = [r_1 \ r_2 \ r_3]^T$ and $\dot{\boldsymbol{r}}_r = \ddot{\boldsymbol{r}}_r = 0$. Also, the two craft on the same side of the center of mass have an angular position $\pm\pi$ radians of the third craft and the angular rates of all three craft are constant with zero acceleration, i.e. $\theta_1 = \theta_2 = \theta_3 \pm \pi$, $\dot{\theta}_1 = \dot{\theta}_2 = \dot{\theta}_3$, and $\ddot{\boldsymbol{\theta}} = 0$. The tracking errors, $\Delta\boldsymbol{r}$, $\Delta\boldsymbol{\theta}$, and $\Delta\boldsymbol{z}$, describe the residuals from the current state to the reference which the Coulomb formation out-of-plane motion is being driven to.

As a result, the tracking errors and respective derivatives are defined as

$$\Delta \boldsymbol{r} = \boldsymbol{r} - \boldsymbol{r}_r \qquad \Delta \dot{\boldsymbol{r}} = \dot{\boldsymbol{r}} - \dot{\boldsymbol{r}}_r = \dot{\boldsymbol{r}} \qquad \Delta \ddot{\boldsymbol{r}} = \ddot{\boldsymbol{r}} - \ddot{\boldsymbol{r}}_r = \ddot{\boldsymbol{r}} \tag{16a}$$

$$\Delta \boldsymbol{\theta} = \boldsymbol{\theta} - \boldsymbol{\theta}_r \qquad \Delta \dot{\boldsymbol{\theta}} = \dot{\boldsymbol{\theta}} - \dot{\boldsymbol{\theta}}_r \qquad \Delta \ddot{\boldsymbol{\theta}} = \ddot{\boldsymbol{\theta}} - \ddot{\boldsymbol{\theta}}_r = \ddot{\boldsymbol{\theta}} \tag{16b}$$

$$\Delta \boldsymbol{z} = \boldsymbol{z} - \boldsymbol{z}_r = \boldsymbol{z} \qquad \Delta \dot{\boldsymbol{z}} = \dot{\boldsymbol{z}} - \dot{\boldsymbol{z}}_r = \dot{\boldsymbol{z}} \qquad \Delta \ddot{\boldsymbol{z}} = \ddot{\boldsymbol{z}} - \ddot{\boldsymbol{z}}_r = \ddot{\boldsymbol{z}} \tag{16c}$$

The in-plane and out-of-plane equations of motion from Eq. (15) are then linearized about the reference trajectory using a Taylor series expansion and dropping higher-order terms.

$$f(\boldsymbol{r}, \boldsymbol{\theta}, \boldsymbol{z}) \approx \frac{\partial f(\boldsymbol{r}, \boldsymbol{\theta}, \boldsymbol{z})}{\partial \boldsymbol{r}}\Big|_{\boldsymbol{r}=\boldsymbol{r}_r} \Delta \boldsymbol{r} + \frac{\partial f(\boldsymbol{r}, \boldsymbol{\theta}, \boldsymbol{z})}{\partial \boldsymbol{\theta}}\Big|_{\boldsymbol{\theta}=\boldsymbol{\theta}_r} \Delta \boldsymbol{\theta} + \frac{\partial f(\boldsymbol{r}, \boldsymbol{\theta}, \boldsymbol{z})}{\partial \boldsymbol{z}}\Big|_{\boldsymbol{z}=\boldsymbol{z}_r} \Delta \boldsymbol{z} \tag{17}$$

The sensitivities of f with respect to the states $\boldsymbol{r}$ and $\boldsymbol{\theta}$ are zero, demonstrating that the out-of-plane $\boldsymbol{z}$ motion indeed decouples to first order from the in-plane motion.

$$\frac{\partial f(\boldsymbol{r}, \boldsymbol{\theta}, \boldsymbol{z})}{\partial \boldsymbol{r}}\Big|_{\boldsymbol{r}=\boldsymbol{r}_r} = \boldsymbol{0} \qquad \frac{\partial f(\boldsymbol{r}, \boldsymbol{\theta}, \boldsymbol{z})}{\partial \boldsymbol{\theta}}\Big|_{\boldsymbol{\theta}=\boldsymbol{\theta}_r} \Delta \boldsymbol{\theta} = \boldsymbol{0} \tag{18}$$

The cylindrical coordinate system chosen provides a natural method to discuss the charged spinning 3-craft motion. Next, of interest is if this out-of-plane motion is stable, and how large it must become before the higher order terms couple the in- and out-of-plane motions again. The linearized out-of-plane equations of motion are

$$f_z(\boldsymbol{r}, \boldsymbol{\theta}, \boldsymbol{z}) \approx [\boldsymbol{A}] \begin{bmatrix} z_1 \\ z_2 \\ z_3 \end{bmatrix} \tag{19a}$$

$$[\boldsymbol{A}(\boldsymbol{r}_r, \boldsymbol{\theta}_r, \boldsymbol{z}_r)] = \begin{bmatrix} \frac{k_c q_1}{m_1}\left(\frac{q_2}{r_{12}^3} + \frac{q_3}{r_{13}^3}\right) & -\frac{k_c q_1 q_2}{m_1 r_{12}^3} & -\frac{k_c q_1 q_3}{m_1 r_{13}^3} \\ -\frac{k_c q_1 q_2}{m_2 r_{12}^3} & \frac{k_c q_2}{m_2}\left(\frac{q_1}{r_{12}^3} + \frac{q_3}{r_{23}^3}\right) & -\frac{k_c q_2 q_3}{m_2 r_{23}^3} \\ -\frac{k_c q_1 q_3}{m_3 r_{13}^3} & -\frac{k_c q_2 q_3}{m_3 r_{23}^3} & \frac{k_c q_3}{m_3}\left(\frac{q_1}{r_{13}^3} + \frac{q_2}{r_{23}^3}\right) \end{bmatrix} \tag{19b}$$

Note that $[A]$ is fully populated, illustrating that while the $\boldsymbol{z}$ motion decouple from the $\boldsymbol{r}$ and θ motion, the individual z_i are still coupled. Further, the evaluation of $[A]$ depends on the equilibrium charges q_i of a particular configuration. For a given configuration, these charges are determined by solving the quintic equation in Eq. (4), not a simple task to do analytically. Thus, the form of $[A]$ is not further reduced, and the following section performs a numerical study to investigate the out-of-plane stability.

Out-of-Plane Stability Analysis

From prior research in Refernece 12, a specific regime of δ and σ can be used to calculate two real roots of the quintic equation for collinear invariant shape Coulomb formations. For a stability analysis of the out-of-plane motion, an eigen decomposition is performed which requires initial conditions for the formation. Tables 1 and 2 list the initial conditions and spacecraft parameters which are used in this paper to describe the collinear invariant shape Coulomb formation. Table 2 lists the mass, m, the initial semi-major axis, r, the initial in-plane angle, θ, and charge, q, of each spacecraft within the Coulomb formation used in this paper. The orbital period of all three craft is approximately 192 minutes.

Table 1. Initial Coulomb Formation Geometry Parameters

δ	σ	χ
-0.05	7	3.2508

Table 2. Initial Spacecraft Parameters

Craft	m [kg]	r [m]	θ [rad]	q [μC]
1	100	44.616	π	10
2	100	19.125	π	1.429
3	100	63.741	0	-200

This χ value of 3.2508 is one root of the quintic equation which exhibits marginal stability for linearized in-plane motion only.[12] To analyze the stability of the out-of-plane dynamics, the linear equations of motion for the z coordinates are considered. Because the system is second order, the z motion is described by

$$\begin{bmatrix} \Delta\dot{\boldsymbol{z}} \\ \Delta\ddot{\boldsymbol{z}} \end{bmatrix} = [B] \begin{bmatrix} \Delta\boldsymbol{z} \\ \Delta\dot{\boldsymbol{z}} \end{bmatrix}, \tag{20}$$

where

$$[B] = \begin{bmatrix} \mathbf{0} & \boldsymbol{I}_{3\times 3} \\ [\boldsymbol{A}(\boldsymbol{r}_r, \boldsymbol{\theta}_r, \boldsymbol{z}_r)] & \mathbf{0} \end{bmatrix}. \tag{21}$$

The eigenvalues of the $[B]$ matrix provide information about the stability of the out-of-plane motion. Here, the conditions listed in Table 2 are used to populate the $[B]$ matrix. Recall that these initial conditions correspond to the $\chi = 3.2508$ invariant shape, which is found to be marginally stable when only in-plane motion is considered.[12] The resulting eigenvalues of the $[B]$ matrix are $\pm 5.5i \cdot 10^{-4}$, $\pm 2.8 \cdot 10^{-4}$, and $\pm 0.0i \cdot 10^{-11}$. The existence of a positive real number eigenvalue indicates that the out-of-plane motion is unstable. That is, any small departure from the nominal $\boldsymbol{z} = \dot{\boldsymbol{z}} = 0$ will result in large deviations. Eventually, the z motion will grow large enough to couple back into the in-plane dynamics and degrade the shape. As long as the departures are small enough, however, the decoupling of the z-motion from the planar motion allows the formation shape to be maintained. In this regime, the out-of-plane motion does not affect the in-plane motion to first order.

This marginally stable root is shown to preserve the formation in-plane motion while the out-of-plane motion remains relatively small compared to the geometry of the Coulomb formation. By initializing the out-of-plane position of crafts 1 and 3 to be zero and perturbing craft 2 with an initial value of 0.001 meter, the uncontrolled Coulomb formation slowly degrades and eventually collapses. Figure 3 shows a three-dimensional view of the simulated formation over a few orbital periods. In this figure, the in-plane position has been projected down to the -100 meter plane in order to visualize the formation degradation while the out-of-plane errors grow. While the out-of-plane errors grow to 10 or 20 meters, the planar invariant-shape is preserved.

While the out-of-plane errors are relatively small, it is acceptable to approximate the higher order terms in the equations of motion to be zero. As a result, the governing motion is described by the linearized equations of motion described in Eq. (19). As the out-of-plane errors grow, the higher

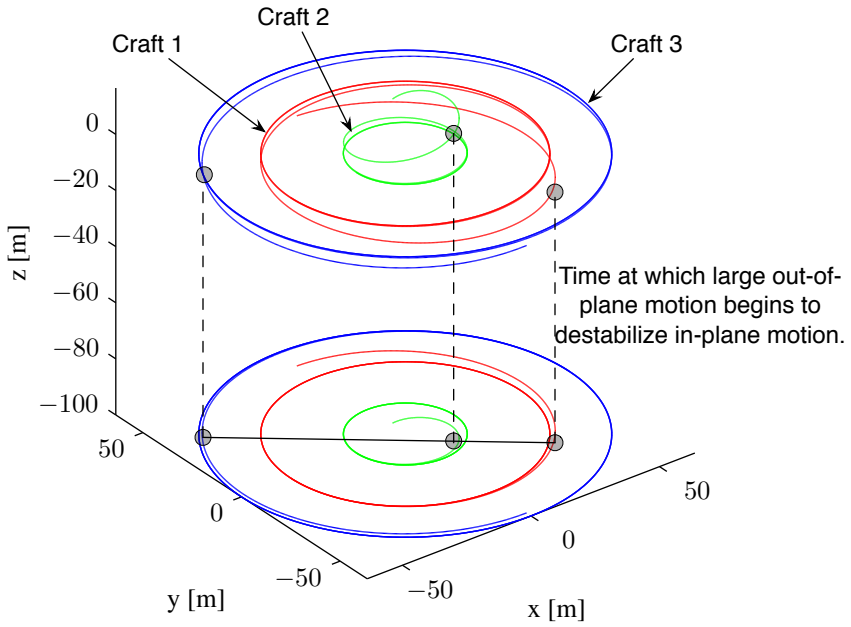

Figure 3. Illustration of Uncontrolled Coulomb Formation Dynamics with Marginally Stable In-Plane Motion

order terms grow and the in-plane motion is coupled with the out-of-plane motion. By controlling the out-of-plane motion, the higher order terms are approximated as zero and the in-plane motion is decoupled from the out-of-plane motion, which preserves the Coulomb formation.

Monte Carlo Analysis of Coulomb Formation Degradation

To obtain information about how different parameters affect the degradation of the planar invariant shape in the presence of out-of-plane perturbations a Monte-Carlo simulation is used to study a wide variety of cases. To determine when the formation has degraded a measure of the quality of the invariant shape is needed. Here χ is used, which is computed using the in-plane projected x and y dimensions. The Monte-Carlo runs are employed to examine the formation behavior under varied initial z perturbations, formation sizes, and orbital periods. For each specified orbital period and formation size, 500 initial z perturbations are applied and the resulting motion of the three craft is determined from numerical integration. The out-of-plane motion is induced by applying a small initial z value to each of the craft. No velocity in the z direction is applied, only a position offset from 0. As the formation size is scaled up, so too are the initial perturbation magnitudes. A normal distribution is used to apply a z perturbation to each craft individually, with a mean of 0 and a standard deviation of $0.0005r_{12}$.

The formation sizes are swept across multiple r_{12} values: 5, 10, 15, 20, and 25 m. For each of these formation sizes, four different orbital periods (P) are considered: 1, 2, 3, and 4 hours. Note that as the orbital period is decreased, higher spin rates occur and larger charge magnitudes are needed to overcome centrifugal effects. For each pair of r_{12} and P, 500 normally distributed initial perturbations are applied, resulting in 10,000 total simulations. To compare the data, the errors in χ are compared with the average magnitude of the z values of all three craft. This average is computed

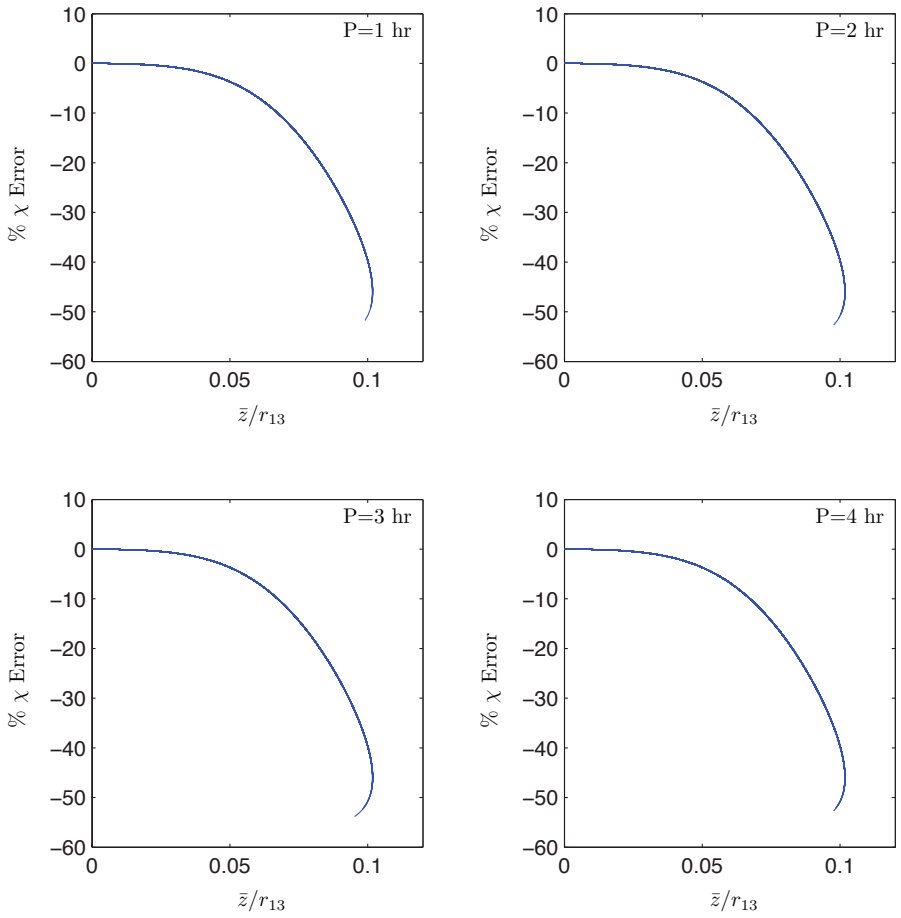

Figure 4. Monte-Carlo results for out-of-plane perturbations

as

$$\bar{z} = (|z_1| + |z_2| + |z_3|)/3. \tag{22}$$

This yields some insight into how much out of plane motion is required before the in-plane projection of the invariant shape degrades. Because various formation sizes are considered, $\bar{z}$ is normalized using the overall dimension of the invariant shape, r_{13}. This allows for a comparison of the data across different formation scales.

The results are presented in Figure 4. These plots are generated by determining $\bar{z}$ and χ from the formation trajectories and plotting the resulting time histories. Two-and-a-half orbital periods of data are used in these plots. Each subplot contains all of the simulations for its corresponding orbital period, including all formation sizes and 500 random initial perturbations. Across all considered orbital periods and formation sizes, the formation degradation follows the same trend. The normalized magnitude of the out-of-plane motion leads to the same percentage errors in χ across all considered cases. These results indicate that the spin-rate and formation size do not greatly influence the out-of-plane instability. While the actual magnitudes of $\bar{z}$ are larger for larger formation sizes, in a normalized sense the trend is equal for all sizes. The invariant shape begins to degrade

when the percent error in χ begins to grow beyond a few percent. For all cases considered here, this corresponds to an average z error of about 5 of the formation size. Thus, for smaller formations a tighter limit exists on how far the out-of-plane motion may grow before the shape begins to degrade. Larger formations may allow for somewhat larger out-of-plane motion, scaled appropriately with the formation size.

Nonlinear Controller Development for Out-of-Plane Motion

As previously stated, the Coulomb formation retains shape within the plane for small out-of-plane deviations. For this reason, the out-of-plane motion of the three craft is controlled in this paper to produce a stable Coulomb formation. This is a nonlinear controller which utilizes the nonlinear equations of motion for the out-of-plane motion described in Eq. (15).

By adding the controller for the out-of-plane motion, $\boldsymbol{u}_z$, the system now looks like

$$\ddot{\boldsymbol{z}} = f(\boldsymbol{r}, \boldsymbol{\theta}, \boldsymbol{z}) + \boldsymbol{u}_z. \tag{23}$$

It is assumed that a relative motion equilibrium has been chosen such that the in-plane motion $(\boldsymbol{r}, \boldsymbol{\theta})$ is marginally stable. The following control does not control these states directly, but assumes they are measurable. Lyapunov's Direct Method[18] is used in this paper to design a nonlinear controller and prove Lyapunov stability for the out-of-plane motion. This method requires the use of a scalar, energy-like Lyapunov function. The Lyapunov function for this analysis is

$$V(\Delta\boldsymbol{z}, \Delta\dot{\boldsymbol{z}}) = \frac{1}{2}\Delta\boldsymbol{z}^T[\boldsymbol{K}_1]\Delta\boldsymbol{z} + \frac{1}{2}\Delta\dot{\boldsymbol{z}}^T\Delta\dot{\boldsymbol{z}}, \tag{24}$$

where $[\boldsymbol{K}_1]$ is a symmetric, positive, definite, matrix related to the out-of-plane position errors. In order for the out-of-plane motion to be Lyapunov stable, $V(\Delta\boldsymbol{z}, \Delta\dot{\boldsymbol{z}})$ is required to have continuous partial derivatives and be a positive definite function about the reference trajectory $\boldsymbol{z}_r$.

A third constraint for Lyapunov stability requires the Lyapunov function rate, $\dot{V}(\Delta\boldsymbol{z}, \Delta\dot{\boldsymbol{z}})$, to be negative semi-definite. The Lyapunov function rate is found by taking the time derivative of the Lyapunov function in Eq. (24).

$$\dot{V}(\Delta\boldsymbol{z}, \Delta\dot{\boldsymbol{z}}) = \Delta\dot{\boldsymbol{z}}^T[\Delta\ddot{\boldsymbol{z}} + [\boldsymbol{K}_1]\Delta\boldsymbol{z}] \tag{25a}$$

$$\dot{V}(\Delta\boldsymbol{z}, \Delta\dot{\boldsymbol{z}}) = \Delta\dot{\boldsymbol{z}}^T[f(\boldsymbol{r}, \boldsymbol{\theta}, \boldsymbol{z}) + \boldsymbol{u}_z - \ddot{\boldsymbol{z}}_r + [\boldsymbol{K}_1]\Delta\boldsymbol{z}] \tag{25b}$$

To ensure the Lyapunov function rate is negative semi-definite, the bracketed term in Eq. (25) is set equal to $-[\boldsymbol{K}_2]\Delta\dot{\boldsymbol{z}}$, where $[\boldsymbol{K}_2]$ is a symmetric, positive, definite matrix related to the out-of-plane velocity errors, so that

$$\dot{V}(\Delta\boldsymbol{z}, \Delta\dot{\boldsymbol{z}}) = -\Delta\dot{\boldsymbol{z}}^T[\boldsymbol{K}_2]\Delta\dot{\boldsymbol{z}} \leq 0 \tag{26}$$

The Lyapunov function rate is only negative semi-definite and not negative definite because $V(\Delta\boldsymbol{z}, \Delta\dot{\boldsymbol{z}})$ is both a function of the position and velocity tracking errors, $\Delta\boldsymbol{z}$ and $\Delta\dot{\boldsymbol{z}}$, and the position tracking error $\Delta\boldsymbol{z}$ is not explicitly present within the $\dot{V}$ expression. The out-of-plane motion is now proven to be Lyapunov stable with the controller, $\boldsymbol{u}_z$, implemented. The controller can be solved for by setting the bracketed term in Eq. (25) equal to $-[\boldsymbol{K}_2]\Delta\dot{\boldsymbol{z}}$,

$$-[\boldsymbol{K}_2]\Delta\dot{\boldsymbol{z}} = f(\boldsymbol{r}, \boldsymbol{\theta}, \boldsymbol{z}) + \boldsymbol{u}_z - \ddot{\boldsymbol{z}}_r + [\boldsymbol{K}_1]\Delta\boldsymbol{z}. \tag{27}$$

Remembering that the reference trajectory is zero, $\boldsymbol{z}_r = \dot{\boldsymbol{z}}_r = \ddot{\boldsymbol{z}}_r = 0$, the controller which produces a Lyapunov stable out-of-plane motion is

$$\boldsymbol{u}_z = -f(\boldsymbol{r}, \boldsymbol{\theta}, \boldsymbol{z}) - [\boldsymbol{K}_1]\Delta\boldsymbol{z} - [\boldsymbol{K}_2]\Delta\dot{\boldsymbol{z}}. \tag{28}$$

While the out-of-plane motion is proven to be Lyapunov stable, it is also proven to exhibit asymptotic stability through the use of the theorem developed by Mukherjee and Chen.[19] Taking higher order derivatives of the Lyapunov function and evaluating them on the set $\Delta\dot{\boldsymbol{z}} = 0$, the first non-zero derivative is found to be

$$\dddot{V}(\Delta\dot{\boldsymbol{z}} = 0) = -2\Delta\boldsymbol{z}^T[K_1]^T[\boldsymbol{K}_2][K_1]\Delta\boldsymbol{z}. \tag{29}$$

Note that this is negative definite in terms of $\Delta\boldsymbol{z}$, proving asymptotic stability.

RESULTS

Application of Nonlinear Controller

To preserve the Coulomb formation for longer periods of time, the nonlinear controller described in Eq. (28) is implemented into a numerical simulation. The gains within the controller, $[\boldsymbol{K}_1]$ and $[\boldsymbol{K}_2]$, are found by critically damping the system and choosing an arbitrary settling time. For a settling time of one hour, $[\boldsymbol{K}_1] = 1.4966 \cdot 10^{-5}\boldsymbol{I}_{3\times3}$ and $[\boldsymbol{K}_2] = 7.7373 \cdot 10^{-3}\boldsymbol{I}_{3\times3}$, where $\boldsymbol{I}_{3\text{x}3}$ is a diagonal identity matrix. The simulation is then run initial out-of-plane position perturbations for crafts 1, 2, and 3 of -2, 2, and -2 meters, respectively. During this simulation, the out-of-plane positions for all three craft are driven to zero. The out-of-plane motion is plotted over time for all three craft on the left side of Figure 5. For the same simulation, the right side of Figure 5 shows the in-plane projection of the Coulomb formation. This simulation numerically proves it is possible to preserve a Coulomb formation for an extended period of time for some specific initial conditions.

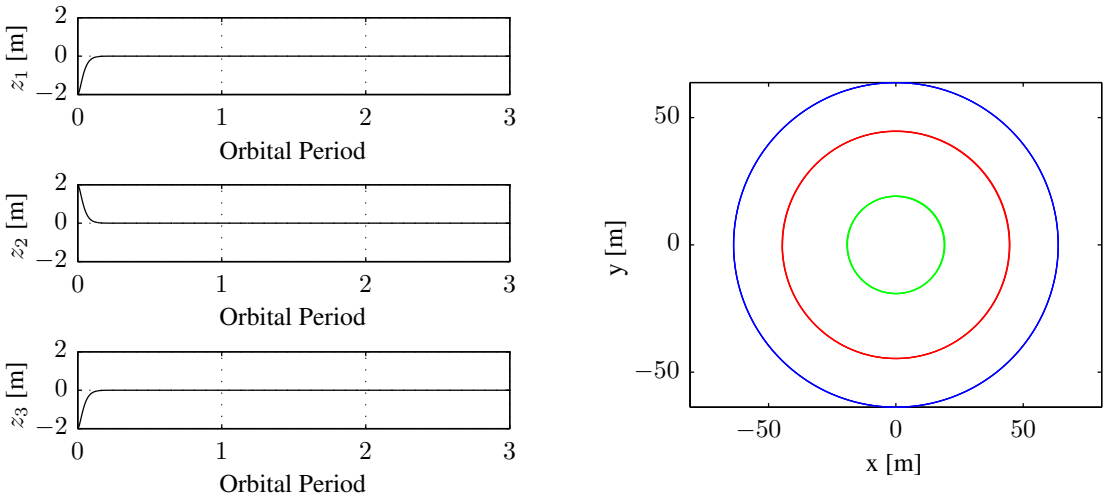

(a) Out-of-Plane (b) In-Plane

Figure 5. Motion of Controlled Coulomb Formation

Deadband Analysis

In real applications, the out-of-plane errors may have some uncertainty due to sensor errors or model errors. To examine this further, a deadband is applied to the nonlinear controller. This restricts the controller from working if the out-of-plane position error is less than a specified amount for any of the three craft. For this simulation, the initial out-of-plane perturbations are set to zero for crafts 1 and 3, while craft 2 is initialized at 0.001 meters. With a settling time of one hour, the controller gains do not change. For this scenario, the simulation is run for ten orbital periods and the largest deadband to produce a stable Coulomb formation, to the nearest tenth of a meter, is ± 3.0 meters. This value was found through a simple trial-and-error analysis. The out-of-plane motion for this case is depicted of the left side of Figure 6 and the projected in-plane motion is shown on the right. These two graphs show the Coulomb formation is preserved while the out-of-plane errors remain relatively small compared to the size of the formation.

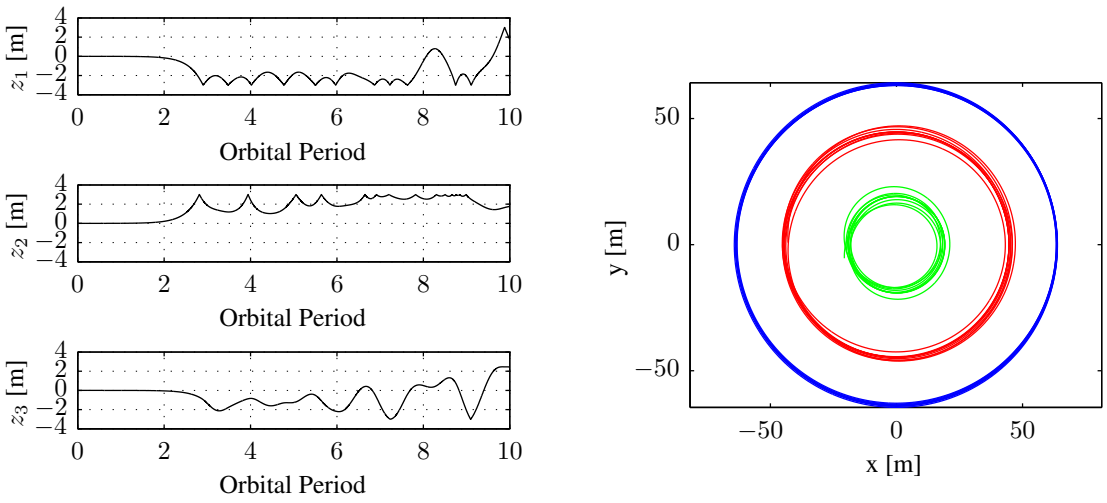

(a) Out-of-Plane (b) In-Plane

Figure 6. Motion of Controlled Coulomb Formation with Settling Time of 1 Hour and a Deadband of ± 3.0 meters

By increasing the settling time to eight hours, the corresponding controller gains decrease to $[\boldsymbol{K}_1] = 2.3385 \cdot 10^{-7}\boldsymbol{I}_{3\times 3}$ and $[\boldsymbol{K}_2] = 9.6716 \cdot 10^{-4}\boldsymbol{I}_{3\times 3}$. With the same initial conditions as before, the largest deadband that maintains the in-plane shape decreases to ± 2.2 meters. The out-of-plane and in-plane motions for this case are depicted in Figure 7.

By varying the settling time and solving for the critically damped gains in the controller, a trend in the deadband is found. Figure 8 shows the data collected from such an analysis. As the settling time increases, the largest allowable deadband decreases. This is due to a smaller force applied to the spacecraft by the controller. With a shorter settling time, the gains within the controller are larger and produce a larger force. This allows the out-of-plane motion to vary more, thus producing a larger allowable deadband. This data seems to dictate that there exists a deadband asymptote value; no matter how large the control input, the higher order terms in the out-of-plane motion will eventually degrade the in-plane shape of the formation.

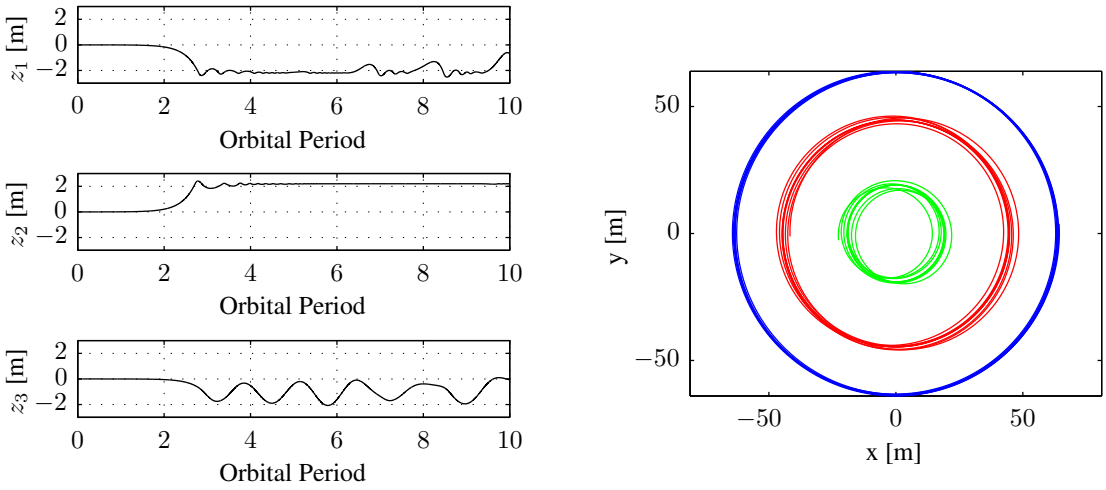

(a) Out-of-Plane (b) In-Plane

Figure 7. Motion of Controlled Coulomb Formation with Settling Time of 8 Hours and a Deadband of $\pm$2.2 meters

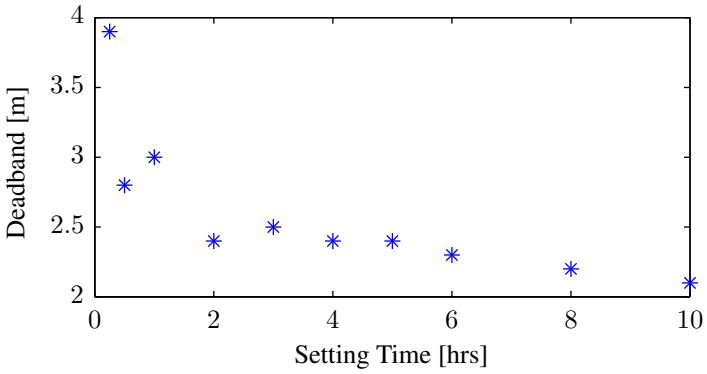

Figure 8. Relationship between System Settling Time and Maximum Deadband Width

CONCLUSION

By implementing a nonlinear controller for the out-of-plane motion the invariant-shape trajectories of the craft in the collinear formation are maintained in the presence of out-of-plane perturbations. The controller acts only on the out-of-plane motion, and is proven to be asymptotically stabilizing. A deadband analysis provides a method to find the largest allowable out-of-plane error for a specified set of controller gains. Once the out-of-plane errors exceed this value, the controller is not able to preserve the Coulomb formation. By critically damping the system and varying the settling time, it is found that the largest allowable deadband is larger for shorter settling times. This is a result of larger forces produced by the controller. A Monte-Carlo analysis shows the spin-rate and formation size do not have a great influence on the out-of-plane instability of a collinear invariant shape Coulomb formation. This produces tighter constraints on the out-of-plane errors in smaller formations and allows larger errors in large formations.

REFERENCES

[1] King, L. B., Parker, G. G., Deshmukh, S., and Chong, J.-H., "Spacecraft Formation-flying using Inter-vehicle Coulomb Forces," Tech. rep., NASA/NIAC, http://www.niac.usra.edu, January 2002.

[2] King, L. B., Parker, G. G., Deshmukh, S., and Chong, J.-H., "Study of Interspacecraft Coulomb Forces and Implications for Formation Flying," *AIAA Journal of Propulsion and Power*, Vol. 19, No. 3, 2003, pp. 497–505.

[3] Lawson, P. R., Lay, O., Johnston, K. J., and Beichman, C. A., "Terrestrial Planet Finder Interferometer Science Working Group," Tech. Rep. JPL Publication 07-1, NASA Jet Propulsion Lab, March 2007.

[4] Cover, J. H., K. W. and Maurer, H. A., "Lightweight Reflecting Structures Utilizing Electrostatic Inflation," .

[5] Pettazzi, L., Izzo, D., and Theil, S., "Swarm navigation and reconfiguration using electrostatic forces," *7th International Conference on Dynamics and Control of Systems and Structures in Space*, The Old Royal Naval College, Greenwich, London, England, 16-20 July 2006.

[6] Dionysiou, D. D. and Stamou, G. G., "Stability of Motion of the Restricted Circular and Charged Three-Body Problem," *Astrophysics and Space Science*, Vol. 152, No. 1, 1989.

[7] Seubert, C. R. and Schaub, H., "Tethered Coulomb Structures: Prospects and Challenges," *Journal of the Astronautical Sciences*, Vol. 57, No. 1-2, Jan.–June 2009, pp. 347–368.

[8] Mullen, E. G., Gussenhoven, M. S., and Hardy, D. A., "SCATHA Survey of High-Voltage Spacecraft Charging in Sunlight," *Journal of the Geophysical Sciences*, Vol. 91, 1986, pp. 1074–1090.

[9] Garrett, H. B., Schwank, D. C., and DeFrost, S. E., "A Statistical Analysis of the Low Energy Geosynchronous Plasma Environment. -I Protons," *Planetary Space Science*, Vol. 29, 1981b, pp. 1045–1060.

[10] Hussein, I. I. and Schaub, H., "Stability and Control of Relative Equilibria for the Three-Spacecraft Coulomb Tether Problem," *Acta Astronautica*, Vol. 65, No. 5-6, 2009, pp. 738–754.

[11] Hogan, E. A. and Schaub, H., "Collinear Invariant Shapes for Three-Craft Coulomb Formations," *2010 AIAA/AAS Astrodynamics Specialists Conference*, Toronto, ON, August 2–5 2010.

[12] Hogan, E. and Schaub, H., "Linear Stability and Shape Analysis of Spinning Three-Craft Coulomb Formations," *AAS Spaceflight Mechanics Meeting*, New Orleans, LA, Feb. 13–17 2011, Paper AAS 11–225.

[13] Hussein, I. I. and Schaub, H., "Invariant Shape Solutions of the Spinning Three Craft Coulomb Tether Problem," *Celestial Mechanics and Dynamical Astronomy*, Vol. 96, No. 2, 2006, pp. 137–157.

[14] Wang, S. and Schaub, H., "Coulomb Control of Nonequilibrium Fixed Shape Triangular Three-Vehicle Cluster," *AIAA Journal of Guidance, Control, and Dynamics*, Vol. 34, No. 1, 2011, pp. 259–270.

[15] Schaub, H. and Hussein, I. I., "Stability and Reconfiguration Analysis of a Circulary Spinning 2-Craft Coulomb Tether," *IEEE Transactions on Aerospace and Electronic Systems*, Vol. 46, No. 4, 2010, pp. 1675–1686.

[16] Alfaro, F. and Perez-Chavela, E., "Linear stability of relative equilibria in the charged three-body problem," *Journal of Differential Equations*, Vol. 245, No. 7, 2008.

[17] Perez-Chavela, E., Saari, D. G., Susin, A., and Yan, Z., "Central Configurations in the Charged Three Body Problem," *Contemporary Mathematics*, Vol. 198, 1995.

[18] Schaub, H. and Junkins, J. L., *Analytical Mechanics of Space Systems*, AIAA Education Series, Reston, VA, 2nd ed., October 2009.

[19] Mukherjee, R. and Chen, D., "Asymptotic Stability Theorem for Autonomous Systems," *Journal of Guidance, Control, and Dynamics*, Vol. 16, Sept. - Oct. 1993, pp. 961–963.